Inorganic Chemistry
Cite This: Inorg. Chem. XXXX, XXX, XXX−XXX
Article
pubs.acs.org/IC

Hydrosilane Synthesis by Catalytic Hydrogenolysis of Chlorosilanes and Silyl Triflates

Arne Glüer,[†] Julia I. Schweizer,[‡] Uhut S. Karaca,[‡] Christian Würtele,[†] Martin Diefenbach,[‡] Max C. Holthausen,*[,‡] and Sven Schneider*[,†]

[†]Institute for Inorganic Chemistry, University of Göttingen, Tammannstraße 4, 37077 Göttingen, Germany
[‡]Institut für Anorganische und Analytische Chemie, Goethe-Universität, Max-von-Laue-Strasse 7, 60438 Frankfurt am Main, Germany

Supporting Information

ABSTRACT: Hydrogenolysis of the chlorosilanes and silyl triflates (triflate = trifluoromethanesulfonate, OTf^-) $Me_{3-n}SiX_{1+n}$ (X = Cl, OTf; n = 0, 1) to hydrosilanes at mild conditions (4 bar of H_2, room temperature) is reported using low loadings (1 mol %) of the bifunctional catalyst $[Ru(H)_2CO(HPNP^{iPr})]$ ($HPNP^{iPr}$ = $HN(CH_2CH_2P(iPr)_2)_2$). Endergonic chlorosilane hydrogenolysis can be driven by chloride removal, e.g., with $NaBAr^F{}_4$ [$BAr^F{}_4^-$ = $B(C_6H_3\text{-}3,5\text{-}(CF_3)_2)_4^-$]. Alternatively, conversion to silyl triflates enables facile hydrogenolysis with NEt_3 as the base, giving Me_3SiH, Me_2SiH_2, and $Me_2SiHOTf$, respectively, in high yields. An outer-sphere mechanism for silyl triflate hydrogenolysis is supported by density functional theory computations. These protocols provide key steps for synthesis of the valuable hydrochlorosilane Me_2SiClH, which can also be directly obtained in yields of over 50% by hydrogenolysis of chlorosilane/silyl triflate mixtures.

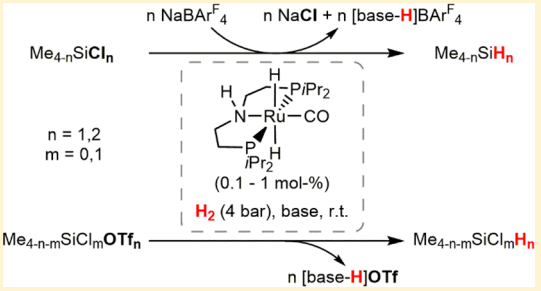

INTRODUCTION

Organohydrosilanes are important reagents for olefin hydrosilylation[1] and other applications such as C−H bond silylation,[2] desulfurization of fuels,[3] or dehydrogenative oligo/polysilane formation.[4] (Organo)hydrochlorosilane building blocks $SiH_xCl_yR_z$ enable the orthogonal synthesis of branched polysiloxanes and self-healing silicones by sequential polycondensation and cross-linking via hydrosilylation as used, e.g., for the fabrication of release coatings, moldings, and adhesives.[5]

Some of these precursors, like $MeSiCl_2H$, are conveniently obtained as byproducts of the Müller−Rochow process. In contrast, Me_2SiClH synthesis suffers from low crude yields (0.01−0.5%, Scheme 1a) and challenging separation procedures, necessitating alternative synthetic routes to hydro(chloro)silanes from chlorosilanes.[6] Hydrosilanes can be prepared by salt metathesis from chlorosilanes with $LiAlH_4$ (Scheme 1b). Besides the low atom economy that is associated with the use of complex hydride reagents, this approach is not commonly applicable for the synthesis of hydrochlorosilanes because of overreduction. Alternatively, partial chlorination of hydrosilanes,[7] e.g., selective $B(C_6F_5)_3$-catalyzed hydrosilane acidolysis, serves as a versatile route to organohydrochlorosilanes (Scheme 1c).[8] However, direct organochlorosilane hydrogenolysis as a source of hydrosilanes remains elusive because of the unfavorable thermochemistry ($Me_3SiCl + H_2 \rightarrow Me_3SiH + HCl$; $\Delta G° = +22.2$ kcal mol^{-1}).[8]

Very recently, Shimada and co-workers pioneered[9] the hydrogenolysis of silyl triflates and halides $R_{3-n}SiX_{n+1}$ with iridium catalysts (Scheme 1d,e).[10] With relatively high catalyst loadings (5−10 mol %) and long reaction times (2−7 days), moderate yields of around 50−60% in Me_2SiH_2 and Me_2SiHCl could be obtained upon hydrogenolysis of Me_2SiOTf_2 [OTf^- = triflate trifluoromethanesulfonate ($O_3SCF_3^-$)] or in situ prepared Me_2SiI_2 and Me_2SiICl, respectively. Guided by our recent work on de/hydrogenation with bifunctional catalysts,[11]

Scheme 1. Synthetic Routes to Hydro(chloro)silanes

a) Müller-Rochow Process:

$$Si + 2\,CH_3Cl \xrightarrow[[Cu]]{590\ K} Me_nSiCl_{4-n} + Disilanes + MeSiCl_2H + Me_2SiClH$$
>90% 1-8% 0.1-5% **0.01-0.5%** (crude yields)

b) Reduction with $LiAlH_4$:

$$R_{4-n}SiCl_n + LiAlH_4 \xrightarrow[-\,AlCl_3]{-\,LiCl} R_{4-n}SiH_n$$
no partial hydrogenation

c) (Partial) Chlorination of Hydrosilanes:

$$R_{4-n}SiH_n \xrightarrow[cat.\ B(C_6F_5)_3]{x\ HCl} R_{4-n}SiCl_xH_{n-x}\quad n = 1\text{-}3$$

d) Hydrogenolysis of Chlorosilanes:

$$R_{4-n}SiCl_n \xrightarrow[C_6H_6/THF]{x\ NaI} R_{4-n}SiCl_{n-x}I_x \xrightarrow[NiPr_2Et,\ 60°C,\ 48h]{[Ir]\ (\mathbf{10\ mol\text{-}\%}),\ H_2} R_{4-n}SiCl_{n-x}H_x$$

e) Hydrogenolysis of Silyl Triflates:

$$R_{4-n}SiOTf_n \xrightarrow[NiPr_2Et,\ r.t.,\ 0.3\text{ - }7d]{[Ir]\ (\mathbf{5\ mol\text{-}\%}),\ H_2} R_{4-n}SiH_n\quad n = 1,2$$

Received: August 17, 2018

DOI: 10.1021/acs.inorgchem.8b02336
Inorg. Chem. XXXX, XXX, XXX−XXX

we here report ruthenium-catalyzed hydrogenolysis of chlorosilanes and silyl triflates with low catalyst loadings.

RESULTS AND DISCUSSION

The considerably higher Si−Cl (~100 kcal mol^{-1}) versus Si−H (~69 kcal mol^{-1}) bond dissociation energy renders hydride versus chloride metathesis a thermochemically challenging step.[12] Therefore, a transition-metal catalyst with low M−H hydridicity[13,14] was targeted, as indicated, e.g., by its capability of catalyzing the hydrogenation of CO_2 to formate [$\Delta G°_H$-(HCO_2^-) = 44 kcal mol^{-1} in MeCN]. Ruthenium MACHO-type catalysts, i.e., [RuCl(H)CO(*H*PNP^R)] [*H*PNP^R = *H*N($CH_2CH_2PR_2$)$_2$], show high activities in CO_2 hydrogenation.[15] A stoichiometric control experiment confirmed that the *trans*-dihydride complex [Ru(H)$_2$(CO)(*H*PNP^{iPr})] (**1**) readily reacts with Me_3SiCl to the corresponding hydrosilane in almost quantitative spectroscopic yield (Scheme 2). This observation also demonstrates favorable kinetics for

Scheme 2. Stoichiometric Hydride Transfer of 1 with Me_3SiCl

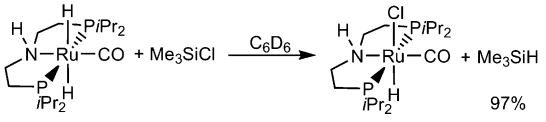

hydride transfer to chlorosilanes with this catalyst class. However, HCl elimination and H_2 heterolysis from the resulting ruthenium chloro complex **2** requires strong bases like alkaline-metal hydroxides, alkoxides, or amides, which all proved to be incompatible with chlorosilane substrates. Accordingly, attempts for the catalytic hydrogenolysis of Me_3SiCl in tetrahydrofuran (THF) with NEt_3 as the base were unsuccessful. Computational evaluation confirmed endergonic hydrogenolysis with the model base NMe_3 (Me_3SiCl + H_2 + NMe_3 → Me_3SiH + [$HNMe_3$]Cl; $\Delta G°$ = 11.9 kcal mol^{-1}), suggesting the requirement of an additional driving force to achieve turnover.

In situ chloride precipitation was therefore evaluated as a synthetic strategy. The addition of NaBAr$^F_4$ [BAr$^F_4{}^-$ = B(C_6H_3-3,5-(CF_3)$_2$)$_4^-$] to complex **2** in PhF as the solvent results in the formation of new species by NMR spectroscopy accompanied by NaCl precipitation (see the Supporting Information, SI). The ^{31}P and ^{1}H NMR spectroscopic and mass (MS) spectrometric data closely resemble the reported values for [Ru(H)CO(*H*PNP^{iPr})]BF_4.[16] Exchange of the solvent with THF-d_8 restores **2**, indicating a strong solvent dependence of the chloride abstraction equilibrium.

Chlorosilane hydrogenolysis (4 bar of H_2, room temperature) with **1** (1 mol %) as the catalyst was therefore examined in the presence of stoichiometric amounts of NaBAr$^F_4$ and excess NEt_3 as the base in PhF. Trimethylchlorosilane as the substrate (Table 1, entry 1) requires relatively long reaction times, giving spectroscopic yields in Me_3SiH around 50% after about 1 week. In contrast, hydrogenolysis of Me_2SiCl_2 (with 2 equiv of NaBAr$^F_4$) to Me_2SiH_2 proceeds at a much faster rate within 1 day in yields up to around 80%[17] under otherwise identical conditions (entry 2), presumably because of the higher electrophilicity of the substrate. With only 1 equiv of NaBAr$^F_4$ (entry 3), Me_2SiH_2 remains the preferred product, leaving almost half of the substrate unreacted. Replacing NEt_3

Table 1. Hydrogenolysis of Chlorosilanes with Catalyst 1[a]

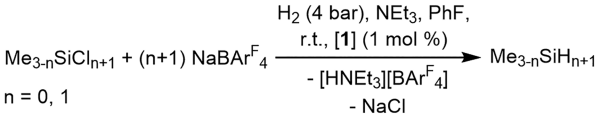

entry	substrate	NaBAr$^F_4$ (equiv)	convn[b] (%)	product (yield[b])	reaction time (h)
1	Me_3SiCl	1.1	77[c]	Me_3SiH (51%)	195
2	Me_2SiCl_2	2.0	100	Me_2SiH_2 (75%)	24
3	Me_2SiCl_2	1.1	59	Me_2SiH_2 (37%)	20

[a]General conditions: 0.027 mmol of chlorosilane, 0.03 or 0.054 mmol of NaBAr$^F_4$, 0.26 μmol of **1**, 0.36 mmol of NEt_3, 0.5 mL of PhF, 4 bar of H_2, room temperature. [b]Conversions/yields were determined by ^{1}H NMR integration of all signals in the Me_xSi region around 0 ppm versus an internal standard (1,2,4,5-tetramethylbenzene). [c]The conversion of [Me_3SiNEt_3][BAr$^F_4$] is given.

by 2,6-lutidine as the base did not give any hydrogenolysis product even after several days under otherwise identical conditions.

Catalytic attempts with other alkaline-metal salts of weakly coordinating anions (WCAs), such as NaOTf, KPF_6, $NaBPh_4$, $NaSbF_6$, or $NaBF_4$, only gave (sub)stoichiometric hydrosilane yields with respect to catalyst loading even at high substrate conversion (see the SI). To clarify the role of the WCAs, the catalytic reaction with NaBAr$^F_4$ was monitored by NMR spectroscopy. The experiment revealed the presence of an intermediate with a ^{29}Si resonance of 47.4 ppm, i.e., characteristic for base-stabilized silyl cations.[18] The same species was obtained upon mixing Me_3SiCl with NaBAr$^F_4$ and NEt_3 in PhF in the absence of catalyst. Furthermore, NEt_3 coordination to silicon is evidenced by a cross peak of the amine methylene protons with the ^{29}Si resonance in the ^{1}H−^{29}Si HMBC NMR spectrum (Figure 1). These results suggest that in situ formed [Me_3SiNEt_3]$^+$ is the actual substrate, which is sufficiently stabilized by the BAr$^F_4{}^-$ anion under catalytic conditions.[19]

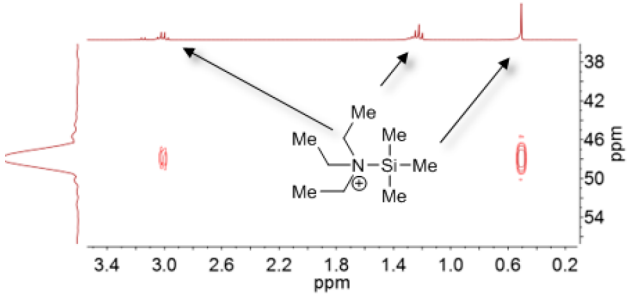

Figure 1. ^{1}H−^{29}Si HMBC NMR spectrum of the product from the reaction of Me_3SiCl with NaBAr$^F_4$ and NEt_3.

Alternative hydrogenolysis strategies were examined to avoid the stoichiometric use of expensive NaBAr$^F_4$ as the chloride scavenger. Silyl triflates can be easily obtained from organochlorosilanes and HOTf with HCl as the only byproduct,[20] possibly providing a better leaving group for catalysis. The reaction of **1** with Me_3SiOTf (1 equiv) in C_6D_6 selectively gives Me_3SiH and [RuH(OTf)CO(*H*PNP^{iPr})] (**3**) by NMR spectroscopy. Complex **3** was independently prepared from **1**

DOI: 10.1021/acs.inorgchem.8b02336
Inorg. Chem. XXXX, XXX, XXX−XXX

with HOTf and fully characterized including single-crystal X-ray diffraction (Figure 2). Importantly, Me_3SiOTf is hydrogenated (1−4 bar of H_2, room temperature) to trimethylsilane in benzene with high yield (>80%) using NEt_3 as the base (Table 2, entries 1−3). Full conversion is obtained overnight with 4 bar of H_2 and 1 mol % catalyst. Almost the same yield is achieved after 46 h with loadings as low as 0.1 mol % **1** (entry 2). A reduction of the H_2 pressure (1.2 bar) gives the same yield with only slighty longer reaction times (entry 3). Hydrogenolysis of $tBuMe_2SiOTf$ was not successful (entry 4) presumably because of steric shielding.

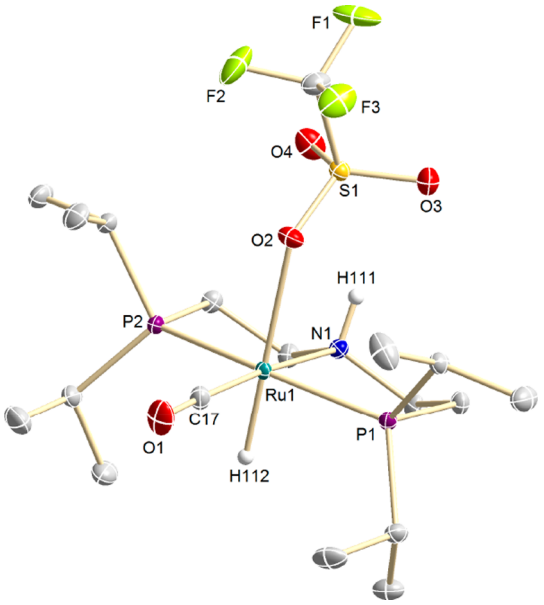

Figure 2. Molecular structure of **3** from single-crystal X-ray diffraction (ellipsoids set at 30% probability; hydrogen atoms, except H111 and H112, omitted for clarity). Selected bond lengths [Å] and angles [deg]: Ru1−C17 1.8320(16), Ru1−N1 2.1969(13), Ru1−O2 2.2957(11), Ru1−P1 2.3195(4), Ru1−P2 2.3276(5), Ru1−H112 1.52(2); C17−Ru1−N1 175.11(6), N1−Ru1−O2 90.82(4), P1−Ru1−P2 164.903(14), O2−Ru1−H112 178.3(8).

Table 2. Hydrogenolysis of Silyl Triflates with Catalyst 1[a]

$Me_{3-n}SiOTf_{n+1}$ —(H_2 (1-4 bar), NEt_3, C_6D_6, r.t., **[1]** (0.1 - 1 mol-%), - $[HNEt_3][OTf]$)→ $Me_{3-n}SiH_{n+1}$

n = 0, 1

entry	substrate	base (equiv)	convn[b] (%)	product (yield[b])	reaction time
1	Me_3SiOTf	NEt_3 (1.1)	99	Me_3SiH (85%)	18 h
2[c]	Me_3SiOTf	NEt_3 (1.1)	92	Me_3SiH (82%)	46 h
3[d]	Me_3SiOTf	NEt_3 (1.0)	90	Me_3SiH (85%)	26 h
4[d]	$tBuMe_2SiOTf$	NEt_3 (1.1)	3	<1%	7 days
5	Me_2SiOTf_2	NEt_3 (2.2)	100	Me_2SiH_2 (82%)	1 h
6	Me_2SiOTf_2	NEt_3 (1.0)	99	$Me_2SiHOTf$ (82%), Me_2SiH_2 (4%)	1 h

[a]General conditions: 0.1 mmol of substrate, 1 μmol of **1**, 4 bar of H_2, 0.5 mL of C_6D_6, room temperature. [b]Conversions/yields were determined by ^1H NMR integration of all signals in the Me_xSi region around 0 ppm versus an internal standard (1,2,4,5-tetramethylbenzene). [c]0.1 μmol of **1** (0.1 mol %). [d]1.2 bar of H_2 was used.

In comparison, double hydrogenolysis of the bistriflate substrate Me_2SiOTf_2 to Me_2SiH_2 is remarkably facile and far more rapid than that with the previously reported iridium catalyst (5 mol % [Ir], 7 days, 53% yield).[10] Full conversion and 82% yield in dihydrosilane is obtained within only 1 h (1 mol % **1**, entry 5). Furthermore, highly selective semihydrogenolysis is obtained within the same time (entry 6) using 1 equiv of base to give $Me_2SiHOTf$ in 82% yield.

During the course of catalysis, **3** is the only ruthenium species observed by ^1H and ^{31}P NMR spectroscopy. After some time, the conjugate acid $[HNEt_3][OTf]$ forms a separate ionic liquid phase, which might be beneficial to driving the reaction (see below). Importantly, the substrate, base, and catalyst remain dissolved in the benzene layer.

Density functional theory calculations were performed for the PMe_2-truncated model system $\mathbf{1^{Me}}$ with NMe_3 as the model base to obtain further insight into the hydrogenolysis mechanism (Scheme 3). Geometry optimizations were performed at the RI-PBE-D3/def2-SVP level of theory. Improved energies were obtained from subsequent SMD-PBE0-D3/def2-TZVP single-point calculations validated against explicitly correlated coupled-cluster energies.[21] The lowest-energy pathway commences with a barrierless endergonic adduct formation between $\mathbf{1^{Me}}$ and Me_3SiOTf to yield intermediate $\mathbf{I1^{Me}}$. Si−O-bond heterolysis proceeds via $\mathbf{ts1^{Me}}$ as the turnover-limiting transition state of the overall process. This leads to exergonic formation of $\mathbf{I2^{Me}}$, which is stabilized by hydrogen bonding of the OTf^- anion to the *H*PNP ligand. Subsequent displacement of Me_3SiH by the triflate anion exhibits a small activation barrier (10 kcal mol^{-1} via $\mathbf{ts2^{Me}}$). The resulting triflate complex $\mathbf{3^{Me}}$ represents the thermodynamic resting state (ΔG° = −10.4 kcal mol^{-1}), in line with the experimental observations (see above). Regeneration of $\mathbf{1^{Me}}$ proceeds without significant barriers and involves H_2 binding to $\mathbf{I3^{Me}}$, followed by base-assisted heterolysis via $\mathbf{ts4^{Me}}$. Overall, hydrogenolysis of Me_3SiOTf and regeneration of the catalyst is computed to be slightly endergonic. This result suggests that the reaction is partially driven by the $[HNMe_3]OTf$ ionic liquid phase separation, which was approximated as an isolated contact ion pair in the computational approach. The effective activation barrier of 25 kcal mol^{-1} is therefore estimated from the energy interval between the resting state $\mathbf{3^{Me}}$ and the rate-limiting $\mathbf{ts1^{Me}}$. This value is in agreement with a reaction that proceeds at room temperature.[22]

The resting state $\mathbf{3^{Me}}$ is stabilized by N−H···OTf hydrogen bonding, as confirmed by the experimental structure of **3** (Figure 2). The N-methylated catalyst $[RuH(OTf)CO(\mathit{Me}PNP^{iPr})]$ [**4**; $\mathit{Me}PNP^{iPr}$ = $\mathit{Me}N(CH_2CH_2PiPr_2)_2$] was therefore employed to probe for rate acceleration by resting-state destabilization. The hydrogenolysis rate of Me_3SiOTf with NEt_3 as the base is, in fact, slightly increased (91% conversion after 130 min) with respect to **3** (81% conversion after 135 min) under identical conditions.

The hydrogenolysis protocols outlined above provide key precursors for facile organohydrochlorosilane synthesis in high yield at mild conditions with low catalyst loadings. Chlorosilyl triflate semihydrogenolysis could be an alternative route for direct synthesis. $Me_2SiClOTf$ can be obtained from Me_2SiCl_2 with 1 equiv of HOTf as the main product according to in situ NMR examination. However, isolation attempts by distillation

DOI: 10.1021/acs.inorgchem.8b02336
Inorg. Chem. XXXX, XXX, XXX−XXX

Scheme 3. Computed Pathway for Hydrogenolysis of Me_3SiOTf Using 1^{Me} [$\Delta G°$ in kcal mol^{-1} (SMD-PBE0-D3/def2-TZVP//RI-PBE-D3/def2-SVP)]

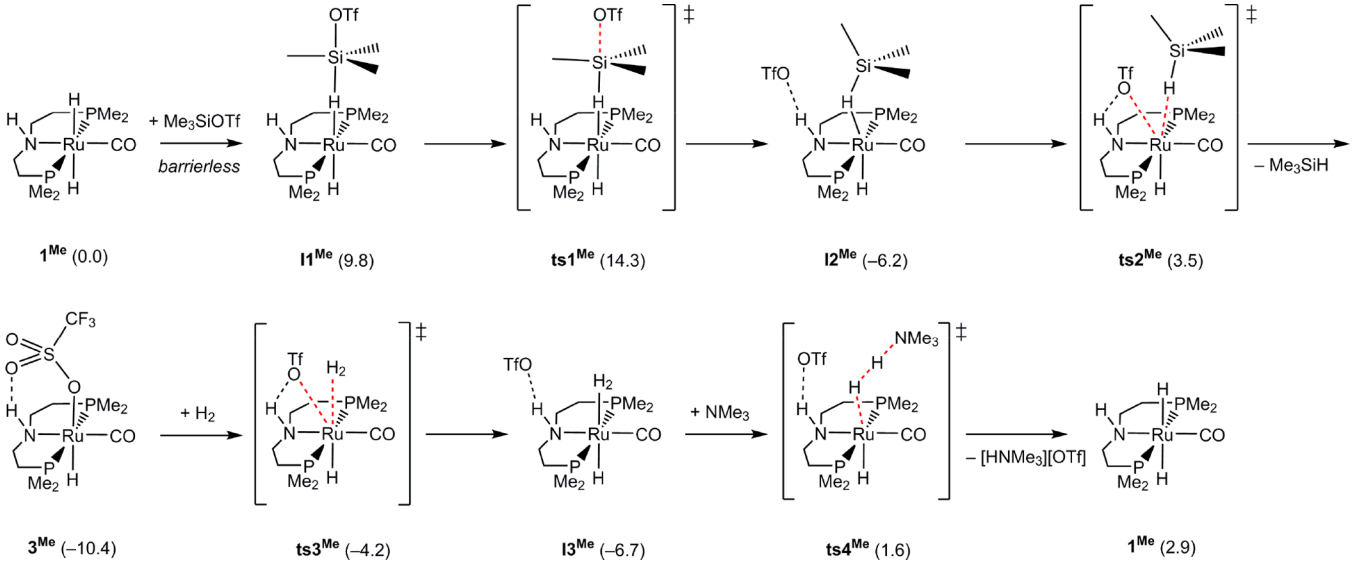

lead to chloride/triflate dismutation (Scheme 4). At room temperature, equilibration is slow (ca. 4 days) but considerably

Scheme 4. Redistribution of Chlorosilanes and Silyl Triflates

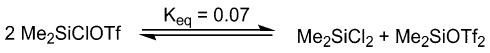

accelerated upon the addition of amines (e.g., NEt_3 or 2,6-lutidine) or **1** (ca. 1 h).[23] Consequently, mixtures of Me_2SiCl_2 and Me_2SiOTf_2 might be directly used after equilibration under catalytic conditions. Rapid (<5 h) full conversion with respect to triflate is obtained with NEt_3 as the base (1 mol % **1**). However, Me_2SiH_2 is the main hydrogenolysis product (36%).[24] The desirable hydrochlorosilane Me_2SiClH is observed only in 5%[24] spectroscopic yield, which could be increased only to 12% using a Me_2SiCl_2/Me_2SiOTf_2 ratio of 5:1 to reduce the Me_2SiOTf_2 equilibrium concentration.

Screening of other ruthenium, iron, and iridium pincer catalysts (see the SI) gave slightly varying dihydrosilane yields. We therefore anticipate kinetic control of the selectivity. Computational evaluation of the Me_2SiCl_2/Me_2SiH_2 dismutation equilibrium, in fact, suggests much higher Me_2SiClH yields under thermodynamic control ($Me_2SiCl_2 + Me_2SiH_2 \rightarrow 2Me_2SiClH$; $\Delta G° = -0.7$ kcal mol^{-1}). In fact, catalytic R_2SiH_2/R_2SiCl_2 dismutation to hydrochlorosilanes has been reported in the literature, and the experimentally derived equilibrium constant for R = Me ($\Delta G°_{exp} \approx -1.3$ kcal mol^{-1}) is in close agreement with our computational estimate.[25]

As a strategy to maintain thermodynamic control, weaker bases than NEt_3 ($pK_{a,MeCN} = 18.8$)[26] were screened. With 2,6-lutidine ($pK_{a,MeCN} = 14.1$)[27] excess base is required for full conversion (97%). Furthermore, Me_2SiClH and 2,6-lutidinium triflate eliminate H_2 under argon, suggesting approximately thermoneutral hydrogenolysis with the conjugate base. High selectivities in Me_2SiClH versus Me_2SiH_2 (>10:1) are obtained for hydrogenolysis of a Me_2SiCl_2/Me_2SiOTf_2 (10:1)[28] mixture with 2,6-lutidine (10 equiv) as the base (Scheme 5). Following the reaction by ^1H NMR (Figure 3) reveals that the reaction is considerably slower than bistriflate hydrogenolysis. Furthermore, the selectivity slightly changes over time in favor of Me_2SiClH. Therefore, high substrate conversion (>90%) and Me_2SiClH yields over 50%[24] require about 1 week under these conditions.

Scheme 5. Hydrogenolysis of a Mixture of Me_2SiCl_2 and Me_2SiOTf_2 with Catalyst 1[24]

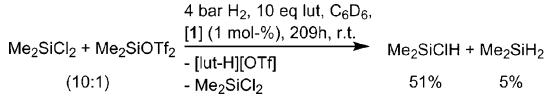

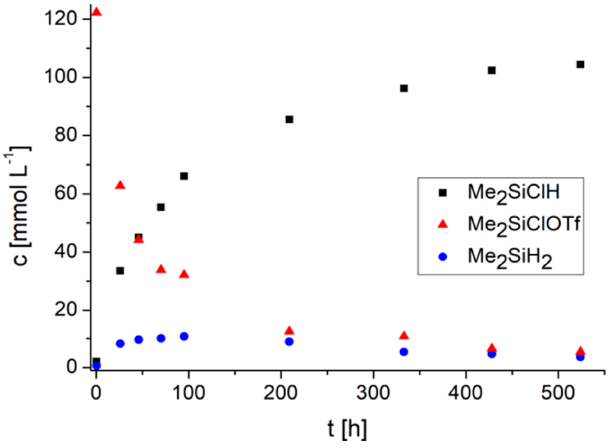

Figure 3. Time-dependent concentration profiles of the reaction depicted in Scheme 5.

In summary, several catalytic hydrogenolysis routes to organohydro- and halohydrosilanes are reported. Mild reaction conditions (1–4 bar of H_2, room temperature) at low catalyst loadings (0.1–1 mol %) and reaction times could be obtained. Especially, bistriflate (semi)hydrogenolysis rapidly affords the organohydrosilane building blocks Me_2SiH_2 and $Me_2SiHOTf$ in excellent yields. Experimental and computational evaluations support a catalytic cycle via outer-sphere hydride transfer and H_2 heterolysis. Chlorosilane hydrogenolysis is enabled by chloride precipitation with $NaBAr^F{}_4$, presumably via base-stabilized silyl cations as key intermediates. In combination,

DOI: 10.1021/acs.inorgchem.8b02336
Inorg. Chem. XXXX, XXX, XXX–XXX

the hydrogenolysis of chlorosilane/silyl triflate mixtures can be optimized to directly give the hydrochlorosilane Me_2SiClH in moderate yields.

EXPERIMENTAL DETAILS

General Information. All experiments were carried out under an argon atmosphere (Linde, 5.0) using Schlenk or glovebox techniques (O_2 and H_2O below 0.1 ppm). NMR tubes were silanized with Me_2SiCl_2, and all glassware was heated in a vacuum prior to use. C_6H_6, Et_2O (stabilized with 2,6-di-*tert*-butyl-4-methylphenol), and pentane (HPLC-grade; Roth, VWR, or Sigma-Aldrich) were degassed and dried by passing through columns packed with activated alumina. Fluorobenzene was degassed and dried over molecular sieves (4 Å). Deuterated solvents were purchased from Deutero GmbH and dried over CaH_2 (CD_2Cl_2) or Na/K (THF-d_8 and C_6D_6) and trap-to-trap transfer in vacuo. NEt_3 was dried over KOH, distilled, and stored over molecular sieves (4 Å). 2,6-Lutidine was dried over $AlCl_3$, distilled, and stored over molecular sieves (4 Å). Me_3SiCl, Me_2SiCl_2, Me_2SiHCl, Me_3SiOTf, *t*$BuMe_2SiOTf$, and MeOTf were degassed and distilled prior to use. 1,2,4,5-Tetramethylbenzene and KO*t*Bu were sublimed prior to use. $NaBPh_4$, $NaBF_4$, $NaSbF_6$, KPF_6, and NaOTf were dried in vacuo prior to use. HOTf (ABCR) was used without further purification. H_2 (Linde, 6.0) was dried by passing through a spiral cooling system, which was immersed in N_2(l). $NaBAr^F{}_4$,[29] 2,6-lutidinium triflate,[30] **1**,[31] and **2**[32] were prepared following published procedures.

NMR spectra were recorded on Bruker Avance III HD 300, 400, or 500 (with broadband cryoprobe) spectrometers and calibrated to the residual proton resonance of the solvent (C_6D_6, δ_H = 7.16 ppm, δ_C = 128.06 ppm; THF-d_8, δ_H = 1.72 ppm/3.58 ppm, δ_C = 25.31 ppm/67.21 ppm; CD_2Cl_2, δ_H = 5.32 ppm, δ_C = 53.84 ppm). ^{31}P and ^{29}Si NMR chemical shifts are reported relative to phosphoric acid (δ_P = 0.0 ppm) and $SiMe_4$ (δ_{Si} = 0.0 ppm), respectively. Signal multiplicities were abbreviated as s (singlet), d (doublet), t (triplet), q (quartet), p (pentet), sept (septet), m (multiplet), and br (broad). Liquid injection field desorption ionization MS (LIFDI-MS) spectra were measured under inert conditions. Elemental analyses were obtained with an Elementar Vario EL 3 analyzer. IR spectra were recorded as powder samples on a Bruker ALPHA FT-IR spectrometer with a platinum ATR module.

Catalytic Protocols. *Hydrogenolysis of Silyl Chlorides.* $NaBAr^F{}_4$, **1**, and the base were dissolved in PhF in a J. Young NMR tube, and the solution was frozen in N_2(l). Chlorosilane was condensed onto the mixture in a static vacuum, and the headspace was refilled with H_2 (1.2 bar). The sample was thawed and immediately shaken. For reactions at 4 bar, the NMR tube was nearly completely immersed in N_2(l) for 1 min during the addition of H_2 before the tube was closed. The products were identified by ^1H and $^1H-^{29}Si$ HMBC NMR spectroscopy and quantified by relative integration of the Me_xSi signals versus an internal standard (1,2,4,5-tetramethylbenzene).

Hydrogenolysis of Pure Silyl Triflates. Silyl triflate, **1**, and the base were dissolved in C_6D_6 in a J. Young NMR tube. The mixture was frozen in N_2(l), and the headspace was evacuated, refilled with H_2 (1.2 bar), and sealed. For reactions at 4 bar, the NMR tube was nearly completely immersed in N_2(l) for 1 min during the addition of H_2 before the tube was closed. The products were identified by ^1H and $^1H-^{29}Si$ HMBC NMR spectroscopy and quantified by relative integration of the Me_xSi signals versus an internal standard (1,2,4,5-tetramethylbenzene).

Hydrogenolysis of Mixtures of Silyl Triflates and Chlorides. Me_2SiOTf_2, Me_2SiCl_2, and the catalyst were dissolved in C_6D_6 in a J. Young NMR tube and shaken for 1.5 h. The base was added, and the NMR tube was frozen in N_2(l). The headspace was evacuated, refilled with H_2 (1.2 bar), and cooled for 1 min. After sealing, the tube was warmed to room temperature, giving a pressure of about 4 bar. The products were identified by ^1H and $^1H-^{29}Si$ HMBC NMR spectroscopy and quantified by relative integration of the Me_xSi signals versus an internal standard (1,2,4,5-tetramethylbenzene).

Synthetic Procedures. *Synthesis of Me_2SiOTf_2.* Me_2SiCl_2 (6.0 mL, 0.05 mol, 1.0 equiv) was stirred at 0 °C and HOTf (12.5 mL, 0.14 mol, 2.8 equiv) added via syringe. The mixture was heated to 60 °C for 2 days with occasional removal of the HCl atmosphere by a stream of argon. Excess acid was neutralized by the careful addition of NEt_3 (8 mL, 0.07 mol, 1.4 equiv) at 0 °C. The removal of volatiles in vacuo and distillation (0.3 mbar, 37 °C) gave Me_2SiOTf_2 as a colorless oil (9 mL, 0.04 mol, 79%) in 97% purity according to ^1H and ^{19}F NMR. ^1H NMR (300.13 MHz, C_6D_6, 300 K): δ −0.01 (s, CH_3). ^{19}F NMR (282.37 MHz, C_6D_6, 298 K): δ −76.66 (s, CF_3). ^{29}Si NMR (59.63 MHz, C_6D_6, 298 K): δ −14.6 (determined by $^1H-^{29}Si$ HMBC).

*Synthesis of [RuH(OTf)CO(HPNP^{iPr})] (**3**).* [$Ru(H)_2CO(HPNP^{iPr})$] (**1**; 100 mg, 0.23 mmol, 1.0 equiv) was dissolved in Et_2O (6 mL) in a J. Young flask, and HOTf (20 μL, 0.23 mmol, 1.0 equiv) was added. The solution was evaporated to 5 mL in vacuo and the precipitated product decanted off. After washing with pentane (3 × 3 mL) and drying in vacuo, crude (99.5% purity) **3** (80 mg, 0.14 mmol, 60%) was obtained as a white solid. After lyophilization, a suspension in Et_2O (0.5 mL) was stirred overnight, decanted off, and dried in vacuo to give **3** as a white solid (75 mg, 0.13 mmol, 56%). Crystals suitable for X-ray crystallography were grown by cooling a saturated Et_2O solution to −40 °C. $^1H\{^{31}P\}$ NMR (500.25 MHz, C_6D_6, 298 K): δ 4.52 (t (br), $^3J_{HH}$ = 11.3 Hz, 1H, N*H*), 2.68 (hept, $^3J_{HH}$ = 7.3 Hz, 2H, CH^{syn}), 2.44 (m, 2H, NCH_2), 1.88 (m, 2H, PCH_2), 1.78 (hept, $^3J_{HH}$ = 6.9 Hz, 2H, C*H*), 1.55 (m, 4H, superposition of PCH_2 and NCH_2), 1.52 (d, $^3J_{HH}$ = 7.3 Hz, 6H, CH_3), 1.03 (d, $^3J_{HH}$ = 6.9 Hz, 6H, $CH_3{}^{anti}$), 1.00 (d, $^3J_{HH}$ = 7.3 Hz, 6H, CH_3), 0.73 (d, $^3J_{HH}$ = 6.9 Hz, 6H, CH_3), −20.9 (s, 1H, Ru−H ($^2J_{HP}$ = 18.0 Hz by ^1H NMR)). $^{13}C\{^1H\}$ NMR (125.80 MHz, C_6D_6, 298 K): δ 205.5 (t, $^2J_{CP}$ = 11.5 Hz, CO), 120.2 (obtained by $^{19}F-^{13}C$ HSQC), 54.0 (vt, N = $|^1J_{CP} + {}^3J_{CP}|$ = 8.8 Hz, NCH_2), 29.6 (vt, N = $|^2J_{CP} + {}^3J_{CP}|$ = 18.5 Hz, PCH_2), 28.1 (vt, N = $|^1J_{CP} + {}^3J_{CP}|$ = 21.6 Hz, *C*H), 23.9 (vt, N = $|^1J_{CP} + {}^3J_{CP}|$ = 26.1 Hz, CH^{anti}), 20.7 (vt, N = $|^2J_{CP} + {}^4J_{CP}|$ = 6.5 Hz, CH_3), 20.1 (vt, N = $|^2J_{CP} + {}^4J_{CP}|$ = 6.5 Hz, CH_3), 18.7 (vt, br, N = $|^2J_{CP} + {}^4J_{CP}|$ = 1.9 Hz, CH_3), 16.9 (vt, N = $|^2J_{CP} + {}^4J_{CP}|$ = 3.5 Hz, CH_3). Assignments were confirmed by 2D NMR. $^{31}P\{^1H\}$ NMR (202.52 MHz, C_6D_6, 298 K): δ 73.8 (s). ^{19}F NMR (470.67 MHz, C_6D_6, 298 K): δ −77.6 (s). LIFDI-MS: *m*/*z* 585.0 (100%; $[M]^+$), 436.1 (80%; $[M - OTf]^+$). IR: ν (cm^{-1}): 3248 (N−H), 2934, 2871, 2035 (Ru−H), 1920 (C≡O), 1879, 1468, 1278, 1231, 1221, 1214, 1188, 1164, 1025, 829, 636, 622. Anal. Calcd for $C_{18}H_{38}F_3NO_4P_2RuS$: C, 36.98; H, 6.55; N, 2.40. Found: C, 37.13; H, 6.42; N, 2.34.

*Synthesis of [RuH(OTf)CO(MePNP^{iPr})] (**4**).* **2** (35.3 mg, 74.3 μmol, 1.0 equiv) and KO*t*Bu (10.1 mg, 90 μmol, 1.2 equiv) were suspended in Et_2O (2 mL) and stirred for 3 h at room temperature. The mixture was filtered through a fritted funnel and the resulting yellow solution dried in vacuo. After extraction with pentane (4 × 4 mL total), MeOTf (8.4 μL, 77 μmol, 1.0 equiv) was added. The precipitated product was filtered off, washed with pentane (3 × 1.5 mL), and extracted with benzene (3 × 0.5 mL). Evaporation of the solvent in vacuo gave **4** as a white powder (33 mg, 74%). Crystals suitable for X-ray crystallography were grown from a saturated solution of Et_2O at −40 °C. $^1H\{^{31}P\}$ NMR (500.25 MHz, C_6D_6, 298 K): δ 2.69 (hept, $^3J_{HH}$ = 7.2 Hz, 2H, CH^{syn}), 2.06 (s, 3H, NCH_3), 1.91−1.82 (m, 4H, NCH^i superposition), 1.79 (hept, $^3J_{HH}$ = 6.9 Hz, 2H, CH^{anti}), 1.60 (d, $^3J_{HH}$ = 7.2 Hz, 6H, CH_3), 1.59−1.51 (m, 2H, $PCH_2{}^{syn}$), 1.43−1.38 (m, 2H, PCH_2), 1.06 (d, $^3J_{HH}$ = 6.9 Hz, 6H, $CH_3{}^{anti}$), 0.97 (d, $^3J_{HH}$ = 7.2 Hz, 6H, CH_3), 0.73 (d, $^3J_{HH}$ = 6.9 Hz, 6H, $CH_3{}^{anti}$), −20.56 (s, 1H, Ru−*H* ($^2J_{HP}$ = 19.0 Hz by ^1H NMR)). $^{13}C\{^1H\}$ NMR (125.80 MHz, C_6D_6, 298 K): δ 205.8 (t, $^2J_{CP}$ = 12.1 Hz, CO), 121.0 (q, $^1J_{CF}$ = 320.1 Hz, CF_3), 65.1 (vt, N = $|^2J_{CP} + {}^3J_{CP}|$ = 9.0 Hz, NCH_2), 45.6 (s, NCH_3), 29.9 (vt, N = $|^1J_{CP} + {}^3J_{CP}|$ = 20.5 Hz, CH^{syn}), 28.1 (vt, N = $|^1J_{CP} + {}^3J_{CP}|$ = 18.0 Hz, PCH_2), 24.3 (vt, N = $|^1J_{CP} + {}^3J_{CP}|$ = 26.6 Hz, *C*), 20.9 (superposition of two vt), N = $|^2J_{CP} + {}^4J_{CP}|$ = 6.0 Hz, CH_3), 19.2 (s, CH_3), 17.1 (vt, N = $|^2J_{CP} + {}^4J_{CP}|$ = 3.5 Hz, CH_3). Assignments were confirmed by 2D NMR. $^{31}P\{^1H\}$ NMR (202.52 MHz, C_6D_6, 298 K): δ 68.8 (s). ^{19}F NMR (470.67 MHz, C_6D_6, 298 K): δ −77.5 (s). LIFDI-MS: *m*/*z* 599.1 (4%; $[M]^+$), 450.2 (100%; $[M - OTf]^+$).

DOI: 10.1021/acs.inorgchem.8b02336
Inorg. Chem. XXXX, XXX, XXX−XXX

IR: ν (cm^{-1}): 2960, 2932, 2873, 2056 (Ru−H), 1917 (C≡O), 1460, 1295, 1235, 1220, 1155, 1032, 882, 821, 695, 633, 518. Anal. Calcd for $C_{19}H_{40}F_3NO_4P_2RuS$: C, 38.12; H, 6.74; N, 2.34. Found: C, 38.05; H, 6.72; N, 2.33.

■ ASSOCIATED CONTENT

Supporting Information

The Supporting Information is available free of charge on the ACS Publications website at DOI: 10.1021/acs.inorgchem.8b02336.

Detailed experimental procedures, characterization of the products, and computational details (PDF)

Accession Codes

CCDC 1855506−1855507 contain the supplementary crystallographic data for this paper. These data can be obtained free of charge via www.ccdc.cam.ac.uk/data_request/cif, or by emailing data_request@ccdc.cam.ac.uk, or by contacting The Cambridge Crystallographic Data Centre, 12 Union Road, Cambridge CB2 1EZ, UK; fax: +44 1223 336033.

■ AUTHOR INFORMATION

Corresponding Authors

*E-mail: max.holthausen@chemie.uni-frankfurt.de.
*E-mail: sven.schneider@chemie.uni-goettingen.de.

ORCID

Max C. Holthausen: 0000-0001-7283-8329
Sven Schneider: 0000-0002-8432-7830

Author Contributions

A.G. performed all synthetic and spectroscopic work while supervised by S.S., and J.I.S., U.S.K., and M.D. carried out the quantum-chemical studies while supervised by M.C.H. Crystallographic characterization was done by C.W. The manuscript was written by A.G., J.I.S., M.C.H., and S.S. All authors commented on the manuscript and approved the final version.

Notes

The authors declare no competing financial interest.

■ ACKNOWLEDGMENTS

The authors thank the European Research Council (Grant 646747) and the Deutsche Forschungsgemeinschaft (CRC 1073, Project C07) for funding and the graduate student program CaSuS (to A.G.). Quantum-chemical calculations were performed at the Center for Scientific Computing (CSC), Frankfurt, Germany, on the FUCHS and LOEWE-CSC high-performance compute clusters. Dr. C. Volkmann is acknowledged for recording parts of the crystallographic data.

■ DEDICATION

This paper is dedicated to Prof. Dr. Dietmar Stalke on the occasion of his 60th birthday.

■ REFERENCES

(1) (a) Park, S.; Chang, S. Catalytic Dearomatization of N-Heteroarenes with Silicon and Boron Compounds. *Angew. Chem., Int. Ed.* **2017**, *56*, 7720. (b) Lipke, M. C.; Liberman-Martin, A. L.; Tilley, T. D. Electrophilic Activation of Silicon−Hydrogen Bonds in Catalytic Hydrosilations. *Angew. Chem., Int. Ed.* **2017**, *56*, 2260. (c) Obligacion, J. V.; Chirik, P. J. Electrophilic Activation of Silicon−Hydrogen Bonds in Catalytic Hydrosilations. *Nat. Rev. Chem.* **2018**, *2*, 15. (d) Chay, R. S.; Rocha, B. G. M.; Pombeiro, A. J. L.; Kukushkin, V. Y.; Luzyanin, K. V. Platinum Complexes with Chelating Acyclic Aminocarbene Ligands Work as Catalysts for Hydrosilylation of Alkynes. *ACS Omega* **2018**, *3*, 863.

(2) (a) Cheng, C.; Hartwig, J. F. Catalytic Silylation of Unactivated C−H Bonds. *Chem. Rev.* **2015**, *115*, 8946. (b) Parasram, M.; Gevorgyan, V. Silicon-Tethered Strategies for C−H Functionalization Reactions. *Acc. Chem. Res.* **2017**, *50*, 2038.

(3) Toutov, A. A.; Salata, M.; Fedorov, A.; Yang, Y.-F.; Liang, Y.; Cariou, R.; Betz, K. N.; Couzijn, E. P. A.; Shabaker, J. W.; Houk, K. N.; Grubbs, R. H. A potassium tert-butoxide and hydrosilane system for ultra-deep desulfurization of fuels. *Nat. Energy* **2017**, *2*, 17008.

(4) (a) Gauvin, F.; Harrod, J. F.; Woo, H.-G. In *Advances in Organometallic Chemistry*; West, R., Hill, A., Eds.; Academic Press, 1998; Vol. *42*, p 363. (b) Waterman, R. Mechanisms of metal-catalyzed dehydrocoupling reactions. *Chem. Soc. Rev.* **2013**, *42*, 5629.

(5) (a) Richards, R. D. C.; Hollingshurst, J.; Semlyen, J. A. Cyclic Polysiloxanes: 5. Preparation and Characterization of poly-(hydrogenmethylsiloxane). *Polymer* **1993**, *34*, 4965. (b) Li, J.; Ren, P.; Zhan, C.; Qin, J. Synthesis and structural characterization of novel multifunctional polysiloxanes having photo-refractive properties. *Polym. Int.* **1999**, *48*, 491. (c) Cancouët, P.; Daudet, E.; Hélary, G.; Moreau, M.; Sauvet, G. Functional polysiloxanes. I. Microstructure of poly(hydrogenmethylsiloxane-co-dimethylsiloxane)s obtained by cationic copolymerization. *J. Polym. Sci., Part A: Polym. Chem.* **2000**, *38*, 826. (d) Beckmann, J.; Dakternieks, D.; Duthie, A.; Foitzik, R. C. The use of Pearlman's catalyst for the oxidation of Si−H bonds. Synthesis, structures and acid-catalysed condensation of novel α,ω-oligosiloxanediols $HOSiMe_2O(SiPh_2O)_nSiMe_2OH$ (n = 1−4). *Silicon Chem.* **2003**, *2*, 27.

(6) Kalchauer, W.; Pachaly, B. In *Handbook of Heterogeneous Catalysis*; Ertl, G., Knözinger, H., Schüth, F., Weitkamp, J., Eds.; Wiley-VCH, 2008; p 2635.

(7) (a) Kunai, A.; Ohshita, J. Selective synthesis of halosilanes from hydrosilanes and utilization for organic synthesis. *J. Organomet. Chem.* **2003**, *686*, 3. (b) Wang, W.; Tan, Y.; Xie, Z.; Zhang, Z. An efficient method to synthesize chlorosilanes from hydrosilanes. *J. Organomet. Chem.* **2014**, *769*, 29.

(8) (a) Chulsky, K.; Dobrovetsky, R. $B(C_6F_5)_3$-Catalyzed Selective Chlorination of Hydrosilanes. *Angew. Chem., Int. Ed.* **2017**, *56*, 4744. (b) Sturm, A. G.; Schweizer, J. I.; Meyer, L.; Santowski, T.; Auner, N.; Holthausen, M. C. Lewis-base catalyzed selective chlorination of monosilanes. *Chem. - Eur. J.* **2018**, DOI: 10.1002/chem.201803921.

(9) Previously, Hidai and co-workers proposed silyl triflate hydrogenolysis as one step in catalytic trimethylsilyl enol ether hydrogenolysis: Nishibayashi, Y.; Takei, I.; Hidai, M.; Takei, I.; Nishibayashi, Y.; Ishii, Y.; Mizobe, Y.; Uemura, S.; Hidai, M. Novel Catalytic Hydrogenolysis of Trimethylsilyl Enol Ethers by the Use of an Acidic Ruthenium Dihydrogen Complex. *Angew. Chem., Int. Ed.* **1999**, *38*, 3047. Takei, I.; Nishibayashi, Y.; Ishii, Y.; Mizobe, Y.; Uemura, S.; Hidai, M. Novel catalytic hydrogenolysis of silyl enol ethers by the use of acidic ruthenium dihydrogen complexes. *J. Organomet. Chem.* **2003**, *679*, 32.

(10) (a) Tsushima, D.; Igarashi, M.; Sato, K.; Shimada, S. Ir-Catalyzed Hydrogenolysis Reaction of Silyl Triflates and Halides with H_2. *Chem. Lett.* **2017**, *46*, 1532. (b) Beppu, T.; Sakamoto, K.; Nakajima, Y.; Matsumoto, K.; Sato, K.; Shimada, S. Hydrosilane Synthesis via Catalytic Hydrogenolysis of Halosilanes Using a Metal-Ligand Bifunctional Iridium Catalyst. *J. Organomet. Chem.* **2018**, *869*, 75.

(11) (a) Käß, M.; Friedrich, A.; Drees, M.; Schneider, S. Ruthenium Complexes with Cooperative PNP Ligands: Bifunctional Catalysts for the Dehydrogenation of Ammonia−Borane. *Angew. Chem., Int. Ed.* **2009**, *48*, 905. (b) Friedrich, A.; Drees, M.; Schneider, S. Ruthenium catalyzed Dimethylamineborane Dehydrogenation: Stepwise Metal Centered Dehydrocyclization. *Chem. - Eur. J.* **2009**, *15*, 10339. (c) Staubitz, A.; Sloan, M. E.; Robertson, A. P. M.; Friedrich, A.; Schneider, S.; Gates, P. J.; Manners, I.; Schmedt auf der Günne, J. Catalytic Dehydrocoupling/Dehydrogenation of N-Methylamine-Borane and Ammonia-Borane: Synthesis and Characterization of High Molecular Weight Polyaminoboranes. *J. Am. Chem. Soc.* **2010**,

DOI: 10.1021/acs.inorgchem.8b02336
Inorg. Chem. XXXX, XXX, XXX−XXX

132, 13332. (d) Marziale, A. N.; Friedrich, A.; Klopsch, I.; Drees, M.; Celinski, V. R.; Schmedt auf der Günne, J.; Schneider, S. The Mechanism of Borane-Amine Dehydrocoupling with Bifunctional Ruthenium Catalysts. *J. Am. Chem. Soc.* **2013**, *135*, 13342. (e) Bielinski, E. A.; Lagaditis, P. O.; Zhang, Y.; Mercado, B. Q.; Würtele, C.; Bernskoetter, W. H.; Hazari, N.; Schneider, S. Lewis Acid-Assisted Formic Acid Dehydrogenation Using a Pincer-Supported Iron Catalyst. *J. Am. Chem. Soc.* **2014**, *136*, 10234. (f) Chakraborty, S.; Lagaditis, P. O.; Förster, M.; Bielinski, E. A.; Hazari, N.; Holthausen, M. C.; Jones, W. D.; Schneider, S. Well-Defined Iron Catalysts for the Acceptorless Reversible Dehydrogenation-Hydrogenation of Alcohols and Ketones. *ACS Catal.* **2014**, *4*, 3994. (g) Glüer, A.; Förster, M.; Celinski, V. R.; Schmedt auf der Günne, J.; Holthausen, M. C.; Schneider, S. Highly Active Iron Catalyst for Ammonia Borane Dehydrocoupling at Room Temperature. *ACS Catal.* **2015**, *5*, 7214. (h) Glüer, A.; Schneider, S. Iron Catalyzed Hydrogenation and Electrochemical Reduction of CO_2: The Role of Functional Ligands. *J. Organomet. Chem.* **2018**, *861*, 159.

(12) Lide, D. R. *CRC Handbook of Chemistry and Physics*; CRC Press, 2005.

(13) The hydridicity ($\Delta G^\circ_{H^-}$) is defined as the free energy of heterolytic M−H bond dissociation: $L_nM{-}H \rightarrow L_nM^+ + H^-$. Better hydride donors are therefore defined by lower hydridicities.

(14) Wiedner, E. S.; Chambers, M. B.; Pitman, C. L.; Bullock, R. M.; Miller, A. J. M.; Appel, A. M. Thermodynamic Hydricity of Transition Metal Hydrides. *Chem. Rev.* **2016**, *116*, 8655.

(15) (a) Liu, Q.; Wu, L.; Gülak, S.; Rockstroh, N.; Jackstell, R.; Beller, M. Towards a Sustainable production of formate salts: Combined catalytic methanol dehydrogenation and bicarbonate hydrogenation. *Angew. Chem., Int. Ed.* **2014**, *53*, 7085. (b) Kothandaraman, J.; Czaun, M.; Goeppert, A.; Haiges, R.; Jones, J. P.; May, R. B.; Prakash, G. K. S.; Olah, G. A. Amine-free reversible hydrogen storage in formate salts catalyzed by ruthenium pincer complex without pH control or solvent change. *ChemSusChem* **2015**, *8*, 1442. (c) Kothandaraman, J.; Goeppert, A.; Czaun, M.; Olah, G. A.; Surya Prakash, G. K. CO_2 capture by amines in aqueous media and its subsequent conversion to formate with reusable ruthenium and iron catalysts. *Green Chem.* **2016**, *18*, 5831.

(16) Alberico, E.; Lennox, A. J. J.; Vogt, L. K.; Jiao, H.; Baumann, W.; Drexler, H.-J.; Nielsen, M.; Spannenberg, A.; Checinski, M. P.; Junge, H.; Beller, M. Unravelling the Mechanism of Basic Aqueous Methanol Dehydrogenation Catalyzed by Ru−PNP Pincer Complexes. *J. Am. Chem. Soc.* **2016**, *138*, 14890.

(17) Besides hydrogenation, hydrolysis products mainly account for the residual conversion.

(18) Lambert, J. B.; Zhang, S.; Ciro, S. M. Silyl Cations in the Solid and in Solution. *Organometallics* **1994**, *13*, 2430.

(19) (a) Emde, H.; Simchen, G. Silylation of nitriles with trimethylsilyl trifluoromethanesulfonate (trimethylsilyl triflate). *Synthesis* **1977**, *9*, 636. (b) Todorova, Z.; Koseva, N.; Troev, K. Sylilation of poly(alkylene H-phosphonate)s - Rapid and efficient method for obtaining poly(alkylene trisilylmethylphosphite)s. *Eur. Polym. J.* **2015**, *62*, 87.

(20) (a) Corey, E. J.; Cho, H.; Rücker, C.; Hua, D. H. Studies with trialkylsilyltriflates: new syntheses and applications. *Tetrahedron Lett.* **1981**, *22*, 3455. (b) Matyjaszewski, K.; Chen, Y. L. Synthesis and reactions of silanes containing two triflate groups. *J. Organomet. Chem.* **1988**, *340*, 7.

(21) See the SI for full computational details.

(22) The effective activation barrier increases slightly for the full *H*PNP^{iPr_2} ligands ($\Delta G^\ddagger$ = 27.6 kcal mol^{-1}; see the SI for details).

(23) The ^{19}F NMR signals for $Me_2SiClOTf$ and Me_2SiOTf_2 collapse to a single resonance upon the addition of a base, evidencing rapid triflate exchange. ^{1}H and ^{1}H−^{29}Si HMBC NMR spectroscopy allow for the unequivocal assignment of all equilibrium species.

(24) Because only Si−OTf bonds are hydrogenated under these conditions, yields and conversions are given with respect to triflate versus 1,2,4,5-tetramethylbenzene as an internal standard.

(25) (a) Stock, A.; Somieski, C. Siliciumwasserstoffe VI. I): Chlorierung und Methylierung des Monosilanes. *Ber. Dtsch. Chem. Ges. B* **1919**, *52*, 695. (b) Whitmore, F. C.; Pietrusza, E. W.; Sommer, L. H. Hydrogen-Halogen Exchange Reactions of Triethylsilane. A New Rearrangement of Neopentyl Chloride. *J. Am. Chem. Soc.* **1947**, *69*, 2108. (c) Weyenberg, D. R.; Bey, A. E.; Ellison, P. J. The tetraalkylammoniumhalide-catalyzed redistribution of hydrogen and chlorine on silicon. *J. Organomet. Chem.* **1965**, *3*, 489. (d) Weyenberg, D. R.; Bey, A.; Stewart, H.; Atwell, W. The redistribution of chlorine, fluorine, or methoxy with hydrogen on silicon. *J. Organomet. Chem.* **1966**, *6*, 583.

(26) Kaljurand, I.; Kütt, A.; Sooväli, L.; Rodima, T.; Mäemets, V.; Leito, I.; Koppel, I. A. Extension of the Self-Consistent Spectrophotometric Basicity Scale in Acetonitrile to a Full Span of 28 pK_a Units: Unification of Different Basicity Scales. *J. Org. Chem.* **2005**, *70*, 1019.

(27) Lõkov, M.; Tshepelevitsh, S.; Heering, A.; Plieger, P. G.; Vianello, R.; Leito, I. On the Basicity of Conjugated Nitrogen Heterocycles in Different Media. *Eur. J. Org. Chem.* **2017**, *2017*, 4475.

(28) Under these conditions, $Me_2SiClOTf$ is the only silyl triflate species detectable by ^{1}H NMR spectroscopy.

(29) Yakelis, N. A.; Bergman, R. G. Safe Preparation and Purification of Sodium Tetrakis[(3,5-trifluoromethyl)phenyl]borate ($NaBAr^F_{24}$): Reliable and Sensitive Analysis of Water in Solutions of Fluorinated Tetraarylborates. *Organometallics* **2005**, *24*, 3579.

(30) Curley, J. J.; Bergman, R. G.; Tilley, T. D. Preparation and physical properties of early-late heterobimetallic compounds featuring Ir−M bonds (M = Ti, Zr, Hf). *Dalton Trans.* **2012**, *41*, 192.

(31) Bertoli, M.; Choualeb, A.; Lough, A. J.; Moore, B.; Spasyuk, D.; Gusev, D. G. Osmium and Ruthenium Catalysts for Dehydrogenation of Alcohols. *Organometallics* **2011**, *30*, 3479.

(32) Han, Z.; Rong, L.; Wu, J.; Zhang, L.; Wang, Z.; Ding, K. Catalytic Hydrogenation of Cyclic Carbonates: A Practical Approach from CO_2 and Epoxides to Methanol and Diols. *Angew. Chem., Int. Ed.* **2012**, *51*, 13041.

DOI: 10.1021/acs.inorgchem.8b02336
Inorg. Chem. XXXX, XXX, XXX−XXX